Determination of Mechanic Resistance of Osseous Element through Finite Element Modeling

E. Isaza[1*], L. García[1], E. Salazar[1]
[1] Department of Mechanical Engineering. Universidad Tecnologica de Pereira. Colombia.
*E-mail: kalios@utp.edu.co

Abstract: in this paper, the geometry and dimensions of a human femur was generated through 3D scanning process, to obtain the femur external topology. The internal structure was obtained through morphological studies based on radiography and tomography, in order to determine the right proportions and dimensions of the internal femur. Then, the complex structure of the femur was represented through three dimensional finite element model, built with Comsol. This model was simulated with isotropic and anisotropic materials, subjected to various mechanical loads according with experimental reference studies. The reference studies, was developed using dual energy X ray absorptiometry (DXA), quantitative computed tomography (QCT) and real human bones, which was subjected to specific loads in order to establish an objective basis for comparison. The main goal of this study is to determine the femur mechanical strength using finite element technique, validating the results by comparison with experimental studies.

Keywords: Finite Element Method, Human Femur Mechanical Behavior, Structural Mechanics Simulation.

1. Introduction

The consequences of hip fracture and femoral fracture are widely known. This phenomenon is one of the principal causes of morbidity among elderly **[1]**. The mechanical strength of the femur varies in every person, but is possible to predict the mechanical resistance with parameters like density, dimensions and mineral content **[4, 5]**. This paper uses different models and empirical studies to determine the mechanical properties of the human femur, developing isotropic and anisotropic models oriented to determine de mechanical behavior of bone. This model gives important information about the resistance of the femur and allows predicting the resistance in function of the specific individual parameters like bone density.

2. CAD model of Femur

2.1 Human Femur Scanning

The first step in the model construction, was de femur topology obtaining. The procedure to obtain the CAE model starts with a femur specimen, which was scanned with a 3D laser scanner. The scanning process delivers a STL file, to be converted in a CAE file. After processing, the STL file becomes a 3D solid model with the external topology of the human femur.

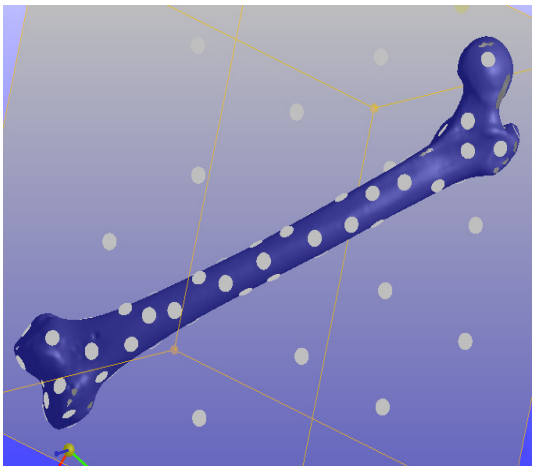

Figure 1: STL model of human femur obtained from 3D scanner.

2.2 CAE Model Obtaining

The mesh obtained from three-dimensional scanning process is the basis for the construction of the solid model of the femur. With the cloud of points obtained proceeded to create surfaces that determine the external shape of the femur.
The obtained surfaces were filled to give solid volume to the model, in order to proceed to generate the internal topology. The used software to generate the CAE model was SolidWorks. With SolidWorks the cloud of points was transformed into surfaces and then in a solid

model. The figure 2 shows the CAE model obtained.

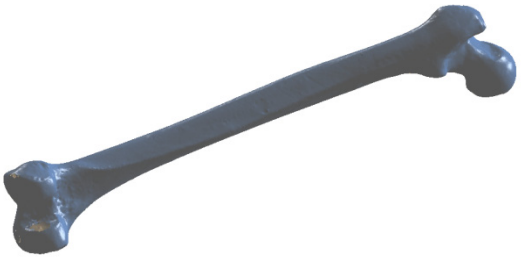

Figure 2: CAE model of human femur.

The next step was the internal modeling of the bone. The human femur is composed mainly of three types of structures, which are referred to as cortical bone, trabecular bone and the medullary canal which houses the bone marrow. Inside the femur are specific distributions of these materials that must be recognized in order to run a proper simulation. The above structures are shown in Figure 3, where it is clearly show the different areas covered by these:

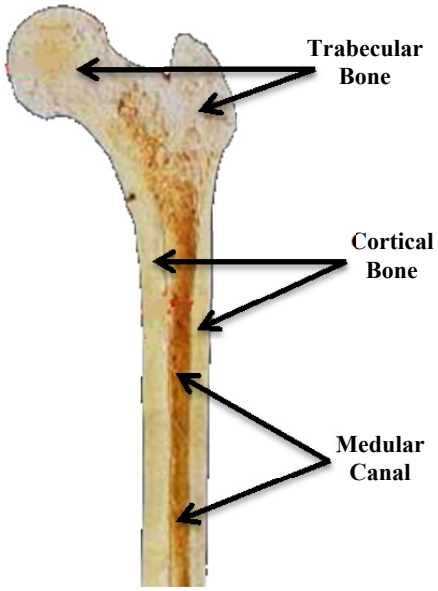

Figure 3: Internal structures of human femur [2]

Determining the boundaries of the structures and proportions of the regions based on the size of the femur is made from X rays and CT studies undertaken by various authors. These studies were summarized in morphological proportions and were characterized in terms of dominant topological parameters as those presented in figure 4:

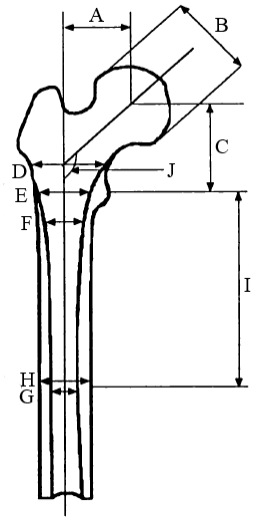

A: femoral head offset
B: femoral head diameter
C: femoral head position
D: canal width above of the lesser trochanter
E: canal width at the level of the lesser trochanter
F: canal width below of the lesser trochanter
G: endosteal width at the isthmus
H: periosteal width at the isthmus
I: isthmus position
J: neck angle

Figure 4: Anatomical characteristics of femur **[3]**

With the introduction of the internal topology of the human femur to CAE model, the geometric construction phase is finished. The final CAE model includes all the external details of the femur obtained through 3D scanning process and the internal configuration derived from studies by X-rays and CT scans. The final version of femur discretized according to the guidelines presented above is illustrated in the figure 5:

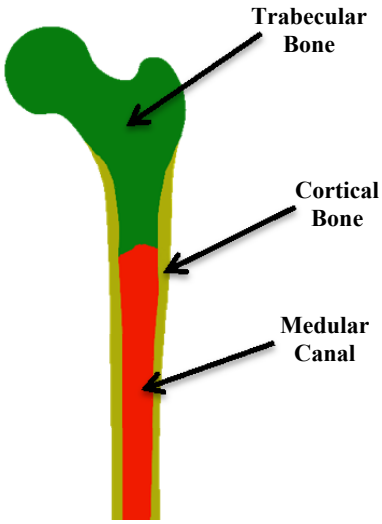

Figure 5: CAE model of human femur with discretized structures.

3. Mechanical Properties of Bone Material.

At this point is important to mention that the transitions between the femur structures are gradual, which in principle could lead to a characterization of the intermediate regions. However, one of the purposes of this study is to determine if a model discretized with only two isotropic materials, and a model consisting of two anisotropic materials, produce results comparable with the results obtained through the load and breakdown of the real bone. The model used for the simulations in Comsol Multiphysics was built with the geometry presented in Figure 5.

3.1 Bone Material Properties

The structures comprising the human femur are mainly cortical bone and trabecular bone. Cortical bone comprises the thinnest part of the bone, connecting the proximal and distal femur. The proximal femur articulates with the hip joint, while the distal femur articulates with the knee. Between these two joint structures is the cortical material. The cortical bone is more dense, compact and rigid, while trabecular bone has a spongy structure which makes it more flexible, less dense, but with a lower mechanical strength. Early studies of the human femur strength assumed total isotropy, generating the first approaches to the performance and resistance of the bone **[7]**. These first models generated an important approach toward understanding the mechanical behavior of the femur; however, it cannot explain why in high stress situations in the middle of the femur, the fractures occur in the intertrochantic area. The recognition of differences between cortical and trabecular bone is fundamental to understand the mechanical behavior of the entire femur.

Trabecular bone has been extensively characterized and studied since its compact structure reflects a more uniform anisotropy, although some authors have taken as an orthotropic material **[4, 6, and 8]**. Table 2 shows exemplary values of the various mechanical properties of cortical bone presented by some authors.

Table 2: mechanical properties of trabecular bone

Mechanical Property	Ashman 1984 [6]	Meunier 1989 [6]	Taylor 2002 [8]
E_1 (GPa)	13.48*	12.41*	17.9
E_2 (GPa)	13.48*	12.41*	18.8
E_3 (GPa)	20.6	20.35	22.8
μ_{12}	0.37	0.41	0.28
μ_{13}	0.22	0.20	0.30
μ_{23}	0.36	0.35	0.31

* Ashman and Meunier developed a model assuming orthotropic behavior.

To understand the meaning of the subindex notation, the figure 6 shows the direction of the axes 1, 2 and 3:

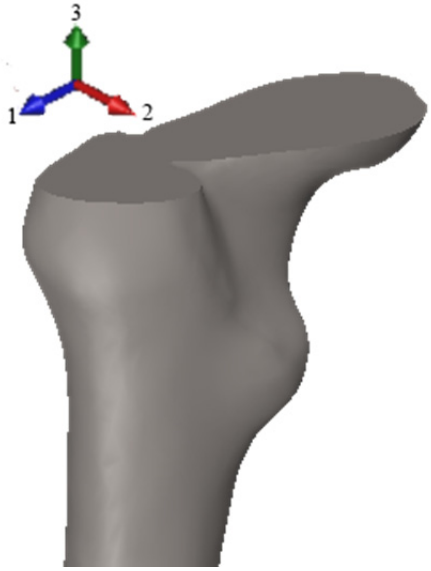

Figure 6: axis direction for Young`s Modulus of the table 2.

3.2 Bone Material Model

To develop the simulations, it was necessary to build a parametric model of the mechanical properties of the trabecular and cortical bones as a function of a specific parameter. The most suitable parameter to guide the mechanical

behavior of the trabecular and cortical bone is the density **[5, 9, and 10]**.

Although studies have found the variation of the mechanical properties of trabecular bone within the bone area **[11, 12]**, we chose to use a model isotropic and anisotropic generalized model for the head of the femur. Similarly made with trabecular structure, however, the variation of the properties of cortical bone along the length of the femur is lower **[13].**

For the isotropic model of trabecular and cortical bone, were used the criteria provided by Wirtz **[5]**. An example of the relationship between density and Young's modulus for the axial load is shown in the figure 6.

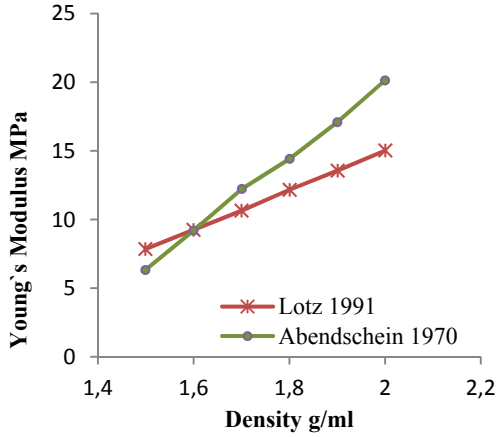

Figure 6: axial Young's modulus for cortical bone **[5]**

For the anisotropic model, the proposals expressed by Rincón **[6]** and Nikodem were used. Rincón presents the stiffness matrix for cortical and trabecular bone as follows:

$$C = \begin{bmatrix} c_{11} & c_{12} & c_{12} & 0 & 0 & 0 \\ c_{12} & c_{11} & c_{12} & 0 & 0 & 0 \\ c_{12} & c_{12} & c_{11} & 0 & 0 & 0 \\ 0 & 0 & 0 & \frac{c_{11}-c_{12}}{2} & 0 & 0 \\ 0 & 0 & 0 & 0 & \frac{c_{11}-c_{12}}{2} & 0 \\ 0 & 0 & 0 & 0 & 0 & \frac{c_{11}-c_{12}}{2} \end{bmatrix}$$

Where:

$$c_{11} = \frac{E}{1-\mu^2} \qquad c_{12} = \frac{\mu . E}{1-\mu^2}$$

In principle, this formulation only require the Young's modulus and Poisson's ratio, however, this matrix can have variations depending on transverse isotropy considerations, overall orthotropy or anisotropy. The orthotropy assumption uses three elastic symmetry planes. For this case the matrix has the following configuration:

$$C = \begin{bmatrix} c_{11} & c_{12} & c_{13} & 0 & 0 & 0 \\ c_{12} & c_{22} & c_{23} & 0 & 0 & 0 \\ c_{13} & c_{23} & c_{33} & 0 & 0 & 0 \\ 0 & 0 & 0 & c_{44} & 0 & 0 \\ 0 & 0 & 0 & 0 & c_{55} & 0 \\ 0 & 0 & 0 & 0 & 0 & c_{66} \end{bmatrix}$$

Some authors referenced by Rincón **[6]**, shown values for the above matrix coefficients found through tests based on ultrasound techniques. These values were used to validate the results reported by Duchemin **[4]**, Rho **[10]** and Nicodem **[14]** in this paper. The table 3 presents the mentioned coefficients. The strength valuesfor cortical and trabecular bone which will prevail to find the breakdown loads, were taken from the studies by Wirtz **[5]** and Nicodem **[14]**. The values of these mechanical properties vary according to the shown behavior in Figure 6. For this cause it was necessary to make a series of simulations varying the density in cortical and trabecular bone.

Table 3: mechanical properties of trabecular bone

GPa	**Van Burskirk 1981[6]**
C_{11}	23.4
C_{33}	32.5
C_{44}	8.71
C_{66}	7.17
C_{12}	9.06
C_{13}	9.11

In table 4 are shown the values of densities and some of the mechanical properties used in the simulations:

Table 4: mechanical properties of trabecular bone obtained from density

Trabecular Density (mg/cm^3)	E_1 (MPa)	E_2 (MPa)	E_3 (MPa)
283,0	449,530	524,120	959,480
434,7	1042,677	1076,308	1651,232
586,4	1635,824	1628,496	2342,984
738,1	2228,971	2180,684	3034,736
889,8	2822,118	2732,872	3726,488
1041,5	3415,265	3285,06	4418,24
1193,2	4008,412	3837,248	5109,992
1344,9	4601,559	4389,436	5801,744
1496,6	5194,706	4941,624	6493,496
1648,3	5787,853	5493,812	7185,248
1800,0	6381,0	6046,0	7877,0

Cortical Density (mg/cm^3)	Tension		Compression	
	E (GPa)	Su (Mpa)	E (GPa)	Su (Mpa)
1000	12,260	85,82	10,30	91,05
1100	13,460	92,22	11,20	100,75
1200	14,660	98,62	12,10	110,45
1300	15,860	105,02	13,00	120,15
1400	17,060	111,42	13,90	129,85
1500	18,260	117,82	14,80	139,55
1600	19,460	124,22	15,70	149,25
1700	20,660	130,62	16,60	158,95
1800	21,860	137,02	17,50	168,65
1900	23,060	143,42	18,40	178,35
2000	24,260	149,82	19,30	188,05

3.3 Loadings and Simulation

In order to have a solid basis for comparison were selected studies by Cody **[15]** based on empirical studies and finite element analysis. In this study the bones was loaded as shown in figure 7. With these parameters we proceeded to do the simulations with different density values extracted from Cody studies. With these data, the failure load delivered by the simulation was plotted over the previous Cody results, generating a visual basis to compare the behavior between the model given by Cody and the isotropic and anisotropic models simulated with Comsol. The plotted results of the simulations and previous Cody results are presented in figure 8.

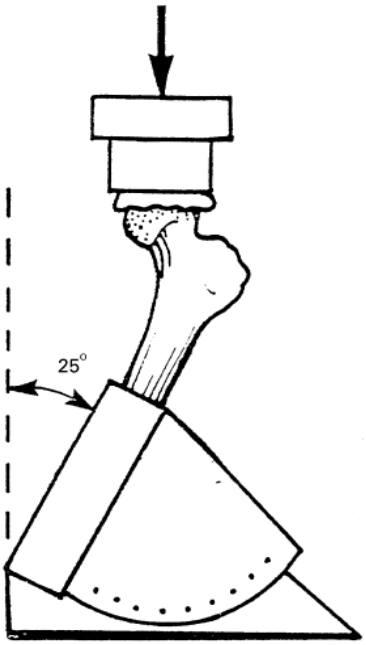

Figure 7: load and fixing for femur simulation

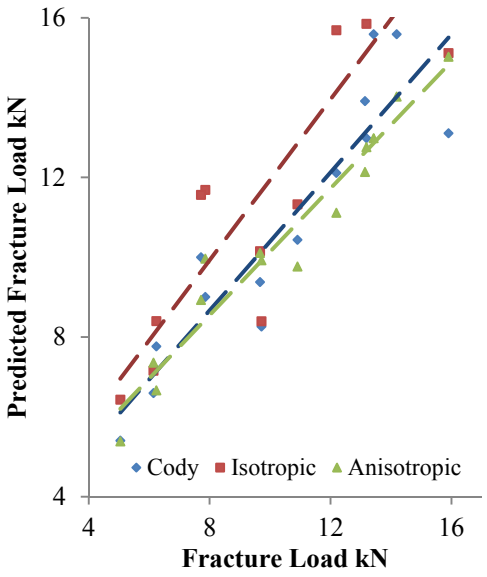

Figure 8: comparison of results from Comsol simulations and empirical results

4. Discussion and Conclusions

The comparison of the results and correlation is presented in the table 5.

Table 5: result comparison

	Cody	Isotropic	Anisotropic
R^2	0.8354	0.6885	0.9123

As is shown in table 5, the correlation obtained by the simulation of the femur with anisotropic material is better. Additionally, the analysis of responses of the isotropic and anisotropic model shows the difference between the stress distributions on the femur head. The principal motivation to study the mechanical resistance of the human femur is to establish a prediction/comparison basis in order to understand de fracture risk for low density bone. For this reason the principal conclusion of this study is the needing to involucrate an anisotropic behavior to predict accurately the breakdown load over the femur.

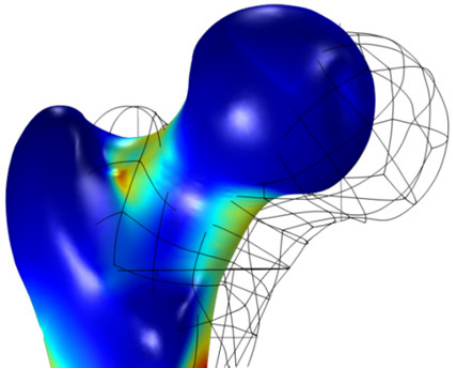

Figure 9: stress in femur head in isotropic model

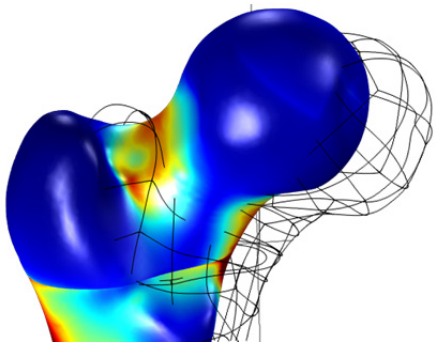

Figure 10: stress in femur head in anisotropic model

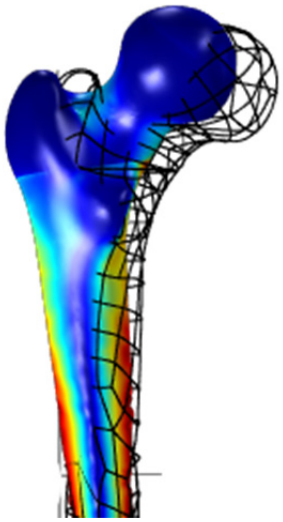

Figure 11: comparative stress distribution between cortical and trabecular bone in human femur.

The figure 11 shows the stress distribution over the head and the neck of the femur. The stress in the femur neck is higher than the stress over the femur head, but, the trabecular bone strength is only the fifth part of the strength of the trabecular bone. This difference guides the behavior of the femur fracture, localized in the intertrochantic zone.

Other conclusion is about Comsol. Comsol Multiphysics allows the implementation of orthotropic and anisotropic materials to simulate with more accurate and realistic parameters. Comsol has a friendly interface and easy to use workflow, winning advantages over other finite elements software. The full customizable conception of the modeling interface, allows the development of specific researches in a wide open fields.

The high resolution finite elements studies give widely accepted results **[12]**, but this study, cheaper and more simply, delivers an acceptable accuracy results without the computing power required for the high resolution finite elements analysis.

5. References

1. D. Testy, M. Viceconti, F. Baruffaldi, A. Capello. Risk of Fracture in Elderly Patients: A New Predictive Index Based on Bone Mineral Density and Finite Element Analysis. *Computer Methods and Programs in Biomedicice,* **Volume 60**, pp. 23-33 (1999).

2. L. Pérez. *Caracterización Sujeto-Específica de las Propiedades Mecánica del Material Óseo en Femur Porcino.* Pontificia Universidad Católica de Chile. Santiago de Chile. (2009)

3. P. Rubin, P. Leyvraz, J. Aubaniac. J. Angenson, P. Estève, B. de Roguin. The Morphology of the Proximal Femur. *The Journa of Bone and Joint Surgery.* **Volume 70-B No I.** pp. 25-32**.** January (1992).

4. L. Duchemin, V. Bousson, C. Raossanaly, C. Bergot, J. Laredo, W. Skally, D. Mitton. Prediction of Mechanical Properties of Cortical Bone by Quantitative Computed Tomography. *Medical Engineering and Physics.* **Volume 30.** pp. 321-328. (2008).

5. D. Wirtz, N. Schiffers, T. Pandorf, K. Randermacher, D. Weichert, R. Forst. Critical Evaluation of Known Material Properties to Realize Anisotropic FE-Simulation of the Proximal Femur. *Journal of Biomechanics.* **Volume 33**. pp. 1325-1330. (2000).

6. E. Rincón, A. Ros, R. Claramunt, F. Arranz. Caracterización Mecánica del Material Óseo. *Tecnología y Desarrollo.* **Volume 2**. pp. 3-27. (2004).

7. R. Huiskes, T. Slooff. Geometrical and Mechanical Properties of the Human Femur. **VI International Congress of Biomechanics, Copenhagen, Denmark.** pp. 57-64. (1977).

8. W. Taylor, E. Roland, H. Ploeg, D. Hertig, R. Klabunde, M. Warner, M. Hobantho, L. Rakotomanana, S. Clift. Determination of orthotropic bone elastic constants using FEA and Modal Analysis. *Journal of Biomechanics.* **Volume 35.** pp. 767-773. (2002).

9. S. Tassani, C. Öhman, F. Baruffaldy, M. Baleani, M. Viceconti. Volume to Density Relation in Adult Human Bone Tissue. *Journal of Biomechanics.* **Volume 44**. pp. 103-108. (2011)

10. J.Rho, M. Hobatho, R. Ashman. Relations of Mechanical Properties to Density and CT Numbers in Human Bone. *Medical Engineering and Physics.* **Volume 17.** pp. 347-355. (1995).

11. T. Brown, A. Ferguson. Mechanical Property Distributions in the Cancellous Bone of the Human Proximal Femur. *Acta Orthop.* **Volume 51**. pp. 429-437. (1980).

12. G. Niebur, M. Felstein, J. Yuen, T. Chen, T. Keaveny. High Resolution Finite Element Models with Tissue Strenght Assimetry Accurately Predict Failure of Trabecular Bone. *Journal of Biomechanics.* **Volume 33**. pp. 1575-1583. (2000).

13. J. Rho, L. Kuhn-Spearing, P. Zioupos. Mechanical Properties and the Hierarchical Structure of Bone. *Medical Engineering and Physics.* **Volume 20.** pp. 92-102. (1997).

14. A. Nikodem. Correlations Between Structural and Mechanical Properties of Human Trabecular Femur Bone. *Acta of Bioengineering and Biomechanics.* **Volume 14 No. 2.** pp. 37-47. (2012).

15. D. Cody, G. Gross, F. Hou, H. Spencer, S. Golstein, D. Fyhrie. Femoral Strength is Better Predicted by Finite Element Models than QCT and DXA. *Journal of Biomechanics.* **Volume 32.** pp. 1013-1020. (1999).